

Spin-Dynamical Analysis of Supercell Spin Configurations

Andrew L. Goodwin,¹ Martin T. Dove,¹ Matthew G. Tucker,² and David A. Keen^{2,3}¹Department of Earth Sciences, Cambridge University, Downing Street, Cambridge CB2 3EQ, U.K.²ISIS Facility, Rutherford Appleton Laboratory, Chilton, Didcot, Oxfordshire OX11 0QX, U.K.³Department of Physics, Oxford University, Clarendon Laboratory, Parks Road, Oxford OX1 3PU, U.K.

(Dated: February 8, 2002)

A model-independent approach capable of extracting spin-wave frequencies and displacement vectors from ensembles of supercell spin configurations is presented. The method is appropriate for those systems whose spin-dynamical motion is well characterised by small-amplitude fluctuations that give harmonic spin waves. The generalised spin coordinate matrix – a quantity that may be calculated from the observed spin orientations in an ensemble of spin configurations – is introduced and its relationship to the spin-dynamical matrix established. Its eigenvalues are subsequently shown to be related to the spin-wave mode frequencies, allowing the extraction of spin-wave dispersion curves from configurational ensembles. Finally, a quantum-mechanical derivation of the same results is given, and the method applied as a case study to spin Monte-Carlo configurations of a 3D Heisenberg ferromagnet.

PACS numbers: 75.30.Ds, 02.70.Ns, 02.70.Ju

I. INTRODUCTION

"Atomistic" simulations of spin interactions in magnetic systems provide a useful mechanism of understanding both structural and dynamical properties of this important class of materials. The reverse Monte-Carlo (RMC) refinement method is a relevant example: a data-driven approach, RMC attempts to account for observed experimental data in terms of ergodic assemblies of atomistic and spin configurations.^{1,2,3} There are a number of established methods of analysing such configurations so as to calculate important thermodynamic quantities;⁴ however, to the best of our knowledge a method of calculating spin-wave dispersion curves in this way has not yet been reported. In this paper, we describe one such method. An important feature of this approach is that spin-dynamical quantities might be extracted from a variety of experimental methods, if these are used to generate the configurations (e.g. by using RMC). Indeed, we have recently applied this approach to reverse Monte-Carlo configurations, allowing extraction of spin-wave dispersion curves from neutron diffraction data.⁵ Our method is appropriate for those systems whose spin-dynamical motion is characterised by small-amplitude fluctuations that give harmonic spin waves. We require harmonicity only at constant temperature; some degree of anharmonic behaviour is allowed in the sense that it is possible to observe changes in spin-wave energies across analyses corresponding to different sample temperatures.

Our paper is arranged as follows. In section II, we first briefly review the well-established concept of the spin-dynamical matrix, re-casting some of the key equations in an appropriate form for our supercell configurational analysis. We then introduce the spin coordinate matrix, which is assembled from the normal mode spin coordinates. We proceed by using this matrix to establish a relationship between the observed orientations in real-space spin configurations and the spin-wave fre-

quencies. Furthermore, we show explicitly how one can then extract spin-wave dispersion curves and spin-wave mode assignments from ensembles of spin configurations, without any prior knowledge of the exchange constants. Finally, we present a derivation of the key results from a quantum-mechanical perspective. In section III, we illustrate the capabilities of the approach through the analysis of configurations generated using a simple spin Monte-Carlo simulation. We show that the method yields the expected spin-wave dispersion relation. Finally, section IV discusses the implementation and some possible extensions of the method.

II. THEORY

A. Semi-classical derivation of the "spin coordinate matrix"

Our theoretical approach builds on the well-established semi-classical theory of spin dynamics (as described, for example in Refs. 6,7,8). Throughout our analysis we will consider only systems with a single spin-alignment axis; however, an extension to multiple-axis systems would be straightforward. Our starting point is the spin-dynamical matrix $\mathbf{D}(\mathbf{k})$, which stores dynamical information in terms of the Heisenberg exchange integrals J . Its rows and columns are indexed by the spin types j , and the corresponding elements are given explicitly by the expression:⁶

$$D_{jj'}(\mathbf{k}) = \frac{1}{2} \sum_{\mathbf{j}''} \frac{J_{j''j}(\mathbf{k})}{J_{j''j}(\mathbf{k})} \frac{J_{j''j'}(\mathbf{k})}{J_{j''j'}(\mathbf{k})} \exp(i\mathbf{k} \cdot \mathbf{r}(\mathbf{j}'') - i\mathbf{k} \cdot \mathbf{r}(\mathbf{j}')) g_{j''}(\mathbf{k}) \quad (1)$$

$$(j, j') \sum_{\mathbf{j}''} \frac{J_{j''j}(\mathbf{k})}{J_{j''j}(\mathbf{k})} \frac{J_{j''j'}(\mathbf{k})}{J_{j''j'}(\mathbf{k})} \exp(i\mathbf{k} \cdot \mathbf{r}(\mathbf{j}'') - i\mathbf{k} \cdot \mathbf{r}(\mathbf{j}')) g_{j''}(\mathbf{k}) :$$

Here, the S_j and $r(j')$ are the spin quantum numbers and average positions, respectively, of each spin j in each unit cell. The eigenvalues of the spin-dynamical matrix are the spin-wave frequencies $\omega(k; \lambda)$, and the right eigenvectors describe the normal mode spin-wave displacements.⁶

We now construct the matrix $\chi(k)$, which we will term the "spin coordinate matrix". It is built from the individual spin orientations produced by the set of spin-wave modes acting on a spin configuration. Two important results will be derived: first, that the spin coordinate matrix is related to the spin-dynamical matrix by the appealing relationship $\chi(k) = kT$ (in the classical limit); second, that the eigenvalues of $\chi(k)$ are the quantities $k_B T = \omega(k; \lambda)$. The latter property is the key result of this paper, as the spin coordinate matrix can be calculated directly from spin configurations, and consequently the spin-wave frequencies can be determined via matrix diagonalisation.

We begin by introducing the magnon variables $(j; k; t)$, $(j; k; t)$. These are defined in terms of the standard spin oscillators S_j^+ and S_j^- :

$$\begin{aligned} (j; k; t) &= \frac{r}{2N} \sum_j S_j^+ \exp[ik \cdot r(j')] \\ (j; k; t) &= \frac{r}{2N} \sum_j S_j^- \exp[-ik \cdot r(j')] \end{aligned}$$

These conjugate variables may be calculated directly for each spin configuration (indexed by the variable t). In particular, they do not rely on any a priori knowledge of the exchange integrals J , nor the number and type of significant interactions for each spin. We proceed by assembling the magnon variables into the column vectors $\chi(k; t)$, $\chi(k; t)$, from which the t -averaged spin coordinate matrix is formed:

$$\chi(k) = \chi(k)^T \chi(k) i:$$

The elements of $\chi(k)$ are given by

$$\chi_{j,j^0}(k) = \frac{r}{2N} \sum_j S_j S_{j^0} \langle h^+(j') + (j^0)^0 i \rangle \exp[ik \cdot (r^0(j) - r(j'))] g: \quad (2)$$

The angular brackets used here represent an average taken either over time (e.g., for spin dynamical (SD) simulations) or over configurations (e.g., for ergodic ensembles). In practice, some degree of error will necessarily be introduced in this process, by considering finite time intervals and/or finitely large configurational ensembles. This error diminishes with the square root of the number of configurations or time steps included in the averaging process.

We proceed to investigate the properties of the matrix $\chi(k)$ further, first forming its product with the spin-dynamical matrix, $\chi(k) \chi(k)$. The diagonal entries of

the product matrix are given explicitly by:

$$[\chi(k) \chi(k)]_{jj} = \sum_{j^0, j^0} S_j S_{j^0} J_{jj^0} \langle h^+(j^0) + (j^0)^0 i \rangle \langle h^+(j^0) + (j^0)^0 i \rangle: \quad (3)$$

The off-diagonal entries $[\chi(k) \chi(k)]_{(i \neq j)}$ contain terms whose exchange integrals $J(i; j^0)$ and spin displacement correlations $\langle h^+(j^0) + (j^0)^0 i \rangle$ do not share like terms; consequently, their time average vanishes. As such, $\chi(k) \chi(k)$ is a diagonal matrix whose diagonal entries are given by Eq. (3).

Within the high-temperature limit, we proceed to show that the diagonal entries are equal to the thermal energy $k_B T$. This is seen by expanding the spin Hamiltonian dot product in terms of the spin variables:

$$S_i \cdot S_j = S_i S_j + \frac{1}{2} (S_i^+ S_j + S_i^- S_j^+ + S_i^+ S_j^- + S_i^- S_j^+):$$

Here we have neglected fourth-order terms in S as | in the limit of small fluctuations | one has $j \cdot j = 1$. Substituting this expansion back into the Hamiltonian,

$$H = \sum_{i \neq j} J(i; j) S_i S_j + \sum_{i \neq j} J(i; j) S_i S_j [S_i^+ S_i + S_i^- S_i^+]: \quad (4)$$

The first term on the right-hand side of this expression corresponds to the spin interaction energy of the system in the absence of any spin excitations, while the second term contains the correction that arises from the population of spin-wave modes. The summation in this spin-wave term runs over all non-trivial pairs $(i; j)$, and so can be separated into contributions H_i from each spin i :

$$H = \sum_{i \neq j} J(i; j) S_i S_j + \sum_i H_i;$$

where

$$H_i = \sum_j J(i; j) S_i S_j [h_i^+ S_i + h_i^- S_i^+]:$$

Here, each Hamiltonian has been replaced by its time average, and so the H_i give the time-averaged thermal energy of each spin i ; in the high-temperature limit this is simply $k_B T$, by the classical equipartition result. A more formal quantum-mechanical treatment is given below; however, the classical result suffices here. By comparison with Eq. (3), one has

$$[\chi(k) \chi(k)]_{jj} = k_B T: \quad (5)$$

This is a key result and gives that the matrix $\chi(k) \chi(k)$ is diagonal with diagonal entries $k_B T$.

One corollary of this result is that the eigenvalues of $\chi(k)$ are the quantities $k_B T = \omega(k; \lambda)$ for each spin-wave mode. This is an important result because the matrix $\chi(k)$ is constructed from the $\chi(k; t)$ and $\chi(k; t)$, the values of which can be determined directly from inspection

of the spin displacements in spin configurations. Consequently, the calculation and diagonalisation of the spin coordinate matrix acts as a model-independent method of extracting spin-wave frequencies from spin configurations.

B. Implementation

In order to assemble a set of spin-wave dispersion curves, one need only calculate $\omega(k)$ for an appropriate range of values of the wave-vector k (corresponding to, for example, the particular reciprocal-space directions of interest). The maximum "resolution" obtainable relies on the number of unit cells represented by each configuration: a supercell containing $n_a; n_b; n_c$ unit cells along axes $a; b; c$ permits the set of wave-vectors:

$$k = \frac{i_a}{n_a}a + \frac{i_b}{n_b}b + \frac{i_c}{n_c}c \quad i_a; i_b; i_c \in \mathbb{Z}$$

Diagonalisation of $\omega(k)$ at each wave-vector then gives the frequencies of the spin-wave modes at that point in reciprocal space. But the method yields more in that the eigenvectors of $\omega(k)$ describe the spin-displacement patterns associated with each normal mode. In this way, the modes may be individually labelled according to their particular displacement pattern, and connected accordingly from k -point to k -point to form the spin-wave dispersion curves. By calculating mode frequencies at symmetry-equivalent wave-vectors, it is possible to estimate the error associated with each point on the curve. Moreover, the acoustic mode frequency at $k = 0$ gives a first-order estimate of the configurational finite-size effects.

It would be possible to extend this analysis through consideration of the implications of lattice symmetry on the form of $\omega(k)$ and $\omega(k)$. By this we mean that one may in principle calculate first the normal mode displacement vectors using standard symmetry arguments, and then use these as a basis in which to express the observed spin displacements. In this representation, the spin displacement matrix would be in block-diagonal form, with each block corresponding to a particular irreducible representation of the point group of the magnetic structure. Individual blocks could then be separated and treated individually, allowing unambiguous identification of the symmetry of each of the normal modes. A similar approach has been applied elsewhere to the analysis of phonon modes from atomic configurations.^{9,10}

C. Quantum-mechanical derivation of the spin coordinate matrix

We now recover the above results from a quantum-mechanical analysis, using standard definitions and notation as described in e.g. Ref.8. For convenience, this derivation is limited to systems that contain only one

spin type; however, the formalisms developed are readily extended to include multiple spin systems. It is easily shown that the spin Hamiltonian can be expressed in terms of the standard magnon creation and annihilation operators $a; a^\dagger$:

$$H = \sum_{i \neq j} J(i; j) S^2 + 2J(i; j) S(a_i a_j - a_i^\dagger a_j^\dagger) :$$

This result holds only under quasi-saturation conditions, where the spin deviations are small.¹² Noting the similarity to Eq. (4), the first term on the right-hand side of this expression represents the energy contribution that arises from the spin alignment process itself (i.e., in the absence of any spin-wave excitations); the second represents the (positive) energy contribution due to thermal excitations of the spins.

We now introduce the Holstein-Primakoff magnon variables,¹¹

$$b_k = \frac{1}{\sqrt{N}} \sum_j a_j \exp(ik \cdot r_j);$$

$$b_k^\dagger = \frac{1}{\sqrt{N}} \sum_j a_j^\dagger \exp(-ik \cdot r_j);$$

which are related to the creation and annihilation operators by reverse Fourier transform:

$$a_j = \frac{1}{\sqrt{N}} \sum_k b_k \exp(-ik \cdot r_j);$$

$$a_j^\dagger = \frac{1}{\sqrt{N}} \sum_k b_k^\dagger \exp(ik \cdot r_j);$$

and can be used as a basis in which to express the spin Hamiltonian. Some manipulation gives

$$H = \sum_{i \neq j} J(i; j) S^2 + \sum_k \tilde{b}_k b_k; \quad (6)$$

where

$$\tilde{b}_k = \frac{2S}{\sqrt{N}} \sum_{i \neq j} J(i; j) [\exp(ik \cdot r_{ji})]$$

and $r_{ji} = r_j - r_i$. Again, it is the second term on the right-hand side of Eq. (6) that arises from the population of spin-wave modes. This expression can in fact be described in terms of the spin-dynamical and spin coordinate matrices as defined above. The identities $a_j = (S+1)^{1/2} +$ and $a_j^\dagger = (S+1)^{1/2} -$ give

$$\tilde{b}_k b_k = \frac{1}{N} \sum_{i, j} a_i a_j \exp(ik \cdot r_{ji})$$

$$= \frac{S}{2N} \sum_{i, j} \exp(ik \cdot r_{ji})$$

$$= \omega(k);$$

Moreover,

$$\begin{aligned} \epsilon_k &= \frac{2S}{N} \sum_{j \neq 0} \mathbf{J}_{j0} \cdot \mathbf{j}_j^0 \\ &= \sum_{j \neq 0} \exp(i\mathbf{k} \cdot \mathbf{r}_j^0) \mathbf{r}_j^0 \cdot \mathbf{j}_j^0 \\ &= \epsilon(k); \end{aligned}$$

by comparison with Eq. (1). Consequently, the Hamiltonian can in fact be written in the form

$$H = \sum_{i,j} \mathbf{J}_{ij} (\mathbf{S}_i \cdot \mathbf{S}_j)^2 + \sum_k \epsilon(k) \sum_{\mathbf{k}} n(\mathbf{k}) \quad (7)$$

The spin-wave energy term in Eq. (7) represents the contribution from thermal population of the individual modes (treating modes at different wave-vectors separately). The final step in the derivation arises from the quantum-mechanical result that the magnon variables give the mode occupation number:⁸ the eigenvalues of $b_k^\dagger b_k$ are the occupation numbers $n(\mathbf{k})$. Consequently the eigenvalues of $\epsilon(\mathbf{k}) = \sum_{\mathbf{k}} b_k^\dagger b_k$ are the values $\sum_{\mathbf{k}} n(\mathbf{k}) \approx k_B T = \epsilon(\mathbf{k})$ (in the high temperature limit). This quantum-mechanical analysis also suggests the diagonalised form of $\epsilon(\mathbf{k})$ (which we denote as $\tilde{\epsilon}(\mathbf{k})$ and $\epsilon(\mathbf{k}) = \tilde{\epsilon}(\mathbf{k})$ when the high-temperature approximations are not used:

$$\epsilon(\mathbf{k}) = \tilde{\epsilon}(\mathbf{k}) = \frac{\sum_{\mathbf{k}} n(\mathbf{k})}{\exp[\tilde{\epsilon}(\mathbf{k})/k_B T] - 1}; \quad (8)$$

giving in turn

$$\epsilon(\mathbf{k}) = \tilde{\epsilon}(\mathbf{k}) = \frac{\sum_{\mathbf{k}} \tilde{\epsilon}(\mathbf{k})}{\exp[\tilde{\epsilon}(\mathbf{k})/k_B T] - 1}; \quad (9)$$

We note that in the high-temperature limit, Eq. (9) reduces to the classical equipartition result cited earlier.

III. CASE STUDY: SPIN MONTE-CARLO SIMULATION OF A 3D $S = \frac{1}{2}$ HEISENBERG FERROMAGNET

In order to test our approach we prepared an ensemble of spin configurations using spin Monte-Carlo simulations. Spin Monte-Carlo is an ideal method for a test case such as this, as one has complete control over the strength and nature of spin interactions, and hence the spin dynamical information reflected in its output. Consequently the form of the spin dispersion that should be recoverable from a configurational ensemble is known precisely. For example, the spin-wave dispersion for a 3D $S = \frac{1}{2}$ Heisenberg ferromagnet is easily shown to be

$$\tilde{\epsilon}(\mathbf{k}) = 4SJ\beta [\cos(ak_x) + \cos(ak_y) + \cos(ak_z)]; \quad (10)$$

Spin Monte-Carlo simulations in which pairs of spins interact via classical ferromagnetic Heisenberg potentials

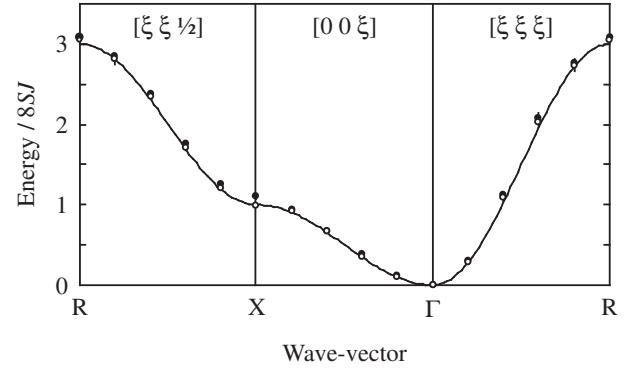


FIG. 1: Spin-wave dispersion curves in a 3D Heisenberg ferromagnet calculated using Eq. (10) (solid line), and extracted from our spin Monte-Carlo simulations using the method developed in the text (open circles| 10 mK; filled circles| 1 K).

should then yield configurations that reflect this same dispersion behaviour.

With this in mind, we generated an ensemble of ca 500 equilibrium Monte-Carlo configurations, each representing a $10 \times 10 \times 10$ supercell of an idealised primitive cubic ferromagnet. The simulation employed a coupling constant $J = 0.4$ meV and was carried out at two temperatures below its paramagnetic phase transition temperature $T_c \approx 3.5$ K: 10 mK and 1 K. We analysed our configurations according to the method described above along the symmetry directions $[\frac{1}{2}]$, $[00]$ and $[\xi\xi\xi]$ at a resolution of 0.1 reciprocal lattice units. In our analysis, it was necessary to account for the classical population statistics inherent to Monte-Carlo simulations, rather than the Bose-Einstein populations implied by Eq. (8). The first-order finite-size effects given by the zone-centre spin-wave frequencies were subtracted from the raw data; these were very small for the $T = 1$ K data, and essentially non-existent for the lower temperature set. The error associated with each point on the dispersion curves was estimated by comparison of the energy values obtained at symmetry-equivalent wave-vectors. Our results are compared with the theoretical dispersion curves in Fig. 1.

The excellent agreement between observed (Monte-Carlo generated spin configuration, analysed via the spin coordinate matrix) and calculated [Eq. (10)] spin-wave dispersion is strong evidence for the applicability of the theoretical approach described in this paper. In this test case, we simply recover the very information that we used to drive the Monte-Carlo simulations—namely the value of J and the nature of the spin interactions. But the key result is that these quantities were extracted solely from a set of individual spin orientations. The analysis is blind to the method with which these were generated, and indeed the particular interaction parameters employed. We have shown that these parameters may be recovered quantitatively from atomistic configurations.

IV. DISCUSSION AND CONCLUSIONS

Our general approach could be automated very easily in the form of a computer program, and our limited experience of implementing the analysis in this way has shown that the calculation of spin-wave dispersion curves of relatively simple systems can be carried out using a conventional desktop computer over very manageable (< 1 h) timescales. The generation of sufficiently many configurations to yield results with acceptable error margins will in general demand significantly more extensive computational resources. We have found that for simple systems, one requires in the vicinity of 500 independent configurations to give acceptable results.

When analysing SD simulations, one has access to more than spin orientations alone, and the use of this additional information can help improve the quality of the spin-wave dispersion curves obtained. Given that the simulations calculate changes in orientation as a function of real time, it is possible to calculate the individual spin momenta across a given configuration. Our method of analysis may be extended by calculating in addition to the spin displacement matrix $\langle \mathbf{r}_i(\mathbf{k}; t) \rangle$ the related spin momentum matrix $\langle \mathbf{p}_i(\mathbf{k}; t) \rangle$, constructed from the momentum variables $\mathbf{p}_i(\mathbf{j}; t)$. Then it is easily shown that the ratio of the eigenvalues $e(\mathbf{k}; \omega)$ of $\langle \mathbf{p}_i(\mathbf{k}; t) \rangle$ to the eigenvalues $e(\mathbf{k}; \omega)$ of $\langle \mathbf{r}_i(\mathbf{k}; t) \rangle$ is related to the spin-wave mode frequencies:

$$\omega^2(\mathbf{k}; \omega) = \frac{e(\mathbf{k}; \omega)}{e(\mathbf{k}; \omega)} : \quad (11)$$

While computationally more intensive, the calculation of spin-wave frequencies in this manner yields results of

a higher quality, particularly in the form of the long-wavelength acoustic modes.¹³ The origin of this improvement is particular to the nature of SD simulations, where the timescale sampled during the simulation might not be sufficient to ensure equipartition of energy between all normal modes. The formalism of Eq. (11) ensures that one evaluates the extent of spin displacement in the context of the population of a particular spin-wave mode, rather than the expected population as given by the overall extent of spin-wave excitation. This extension is of course irrelevant in the analysis of ergodic simulations, where there is no real concept of time.

In conclusion, we have shown how a relatively straightforward extension of standard spin-wave theory can be used to obtain a quantitative link between the energies of the various spin-wave modes in a material and the individual spin orientations one might observe in "atomistic" models of its behaviour. The method we describe has the particular advantage that it allows the extraction of spin-dynamical quantities without any prior assumption of the form of the various spin interactions. This model-independence would be of significant advantage when using the technique to study materials for which little is known a priori about the nature of the magnetic interactions, or where one wishes to avoid the presumption of a particular interaction model.

Acknowledgements

We acknowledge financial support from the EPSRC (UK), and from Trinity College, Cambridge to A.L.G. We thank Dr A.T. Boothroyd for helpful discussions.

¹ D.A. Keen, R.L. McGreevy, J. Phys.: Condens. Matter 3, 7383 (1991).

² A. Møllergaard, R.L. McGreevy, Chem. Phys. 261, 267 (2000).

³ A.L. Goodwin, M.G. Tucker, M.T. Dove, D.A. Keen, Phys. Rev. Lett. 96, 047209 (2006).

⁴ D.P. Landau, M. Krech, J. Phys.: Condens. Matter 11, R179 (1999).

⁵ A.L. Goodwin, M.T. Dove, M.G. Tucker, D.A. Keen, arXiv:cond-mat/0601558 (unpublished).

⁶ F. Keffer, Handb. Phys. 18 (II), 1 (1966).

⁷ N. Ashcroft and N.D. Mermin, Solid State Physics (Holt-Saunders Japan, Ltd., Tokyo, 1976).

⁸ C. Kittel, Quantum Theory of Solids (John Wiley & Sons, New York, 1987).

⁹ F.S. Tautz, V. Heine, M.T. Dove, X. Chen, Phys. Chem. Min. 18, 326 (1991).

¹⁰ A.L. Goodwin, M.G. Tucker, E.R. Cope, M.T. Dove, D.A. Keen, Phys. Rev. B 72, 214304 (2005).

¹¹ T. Holstein and H. Primakoff, Phys. Rev. 58, 1098 (1940).

¹² An analogous approximation was used in the quasi-classical treatment given above, when assuming $j \ll j_1$.

¹³ M.T. Dove, Introduction to Lattice Dynamics (Cambridge University Press, Cambridge, England, 1993).